

# Newly Synthesized Indolylacetic Derivatives Reduce Tumor Necrosis Factor-Mediated Neuroinflammation and Prolong Survival in Amyotrophic Lateral Sclerosis Mice

Angela Corvino, Giuseppe Caliendo, Ferdinando Fiorino, Francesco Frecentese, Valeria Valsecchi, Giovanna Lombardi, Serenella Anzilotti, Giorgia Andreozzi, Antonia Scognamiglio, Rosa Sparaco, Elisa Perissutti, Beatrice Severino, Michele Gargiulo, Vincenzo Santagada, and Giuseppe Pignataro\*



Cite This: *ACS Pharmacol. Transl. Sci.* 2024, 7, 1996–2005

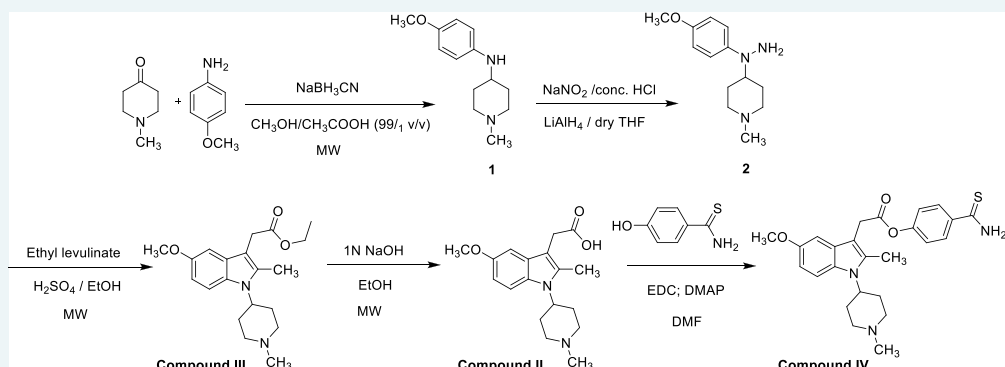


Read Online

ACCESS |

Metrics & More

Article Recommendations



**ABSTRACT:** The debilitating neurodegenerative disease known as amyotrophic lateral sclerosis (ALS) is characterized by the progressive loss of motor neurons (MNs) in the brain, spinal cord, and motor cortex. The ALS neuroinflammatory component is being characterized and includes the overexpression of mediators, such as inducible nitric oxide synthase (iNOS) and tumor necrosis factor- $\alpha$  (TNF- $\alpha$ ). Currently, there are no effective treatments for ALS. Indeed, riluzole, an N-methyl-D-aspartate (NMDA) glutamate receptor blocker, and edaravone, a reactive oxygen species (ROS) scavenger, are currently the sole two medications approved for ALS treatment. However, their efficacy in extending life expectancy typically amounts to only a few months. In order to improve the medicaments for the treatment of neurodegenerative diseases, preferably ALS, novel substituted 2-methyl-3-indolylacetic derivatives (compounds II–IV) were developed by combining the essential parts of two small molecules, namely, the opioids containing a 4-piperidinyl ring with indomethacin, previously shown to be efficacious in different experimental models of neuroinflammation. The synthesized compounds were evaluated for their potential capability of slowing down neurodegeneration associated with ALS progression in preclinical models of the disease in vitro and in vivo. Notably, we produced data to demonstrate that the treatment with the newly synthesized compound III: (1) prevented the upregulation of TNF- $\alpha$  observed in BV-2 microglial cells exposed to the toxin lipopolysaccharides (LPS), (2) preserved SHSY-5Y cell survival exposed to  $\beta$ -N-methylamino-L-alanine (L-BMAA) neurotoxin, and (3) mitigated motor symptoms and improved survival rate of SOD1G93A ALS mice. In conclusion, the findings of the present work support the potential of the synthesized indolylacetic derivatives II–IV in ALS treatment. Indeed, in the attempt to realize an association between two active molecules, we assumed that the combination of the indispensable moieties of two small molecules (the opioids containing a 4-piperidinyl ring with the FANS indomethacin) might lead to new medicaments potentially useful for the treatment of amyotrophic lateral sclerosis.

**KEYWORDS:** ALS, neuroinflammation, indolylacetic derivatives, TNF- $\alpha$

## 1. INTRODUCTION

The debilitating neurodegenerative disease known as amyotrophic lateral sclerosis (ALS) is characterized by the progressive loss of motor neurons (MNs) in the brainstem, spinal cord, and motor cortex.<sup>1</sup> The disease often manifests at its peak between 45 and 60 years of age, with a 3–5 year

Received: February 20, 2024

Revised: June 7, 2024

Accepted: June 11, 2024

Published: June 22, 2024



postdiagnosis survival period. However, ALS may manifest a clinically diverse pathophysiology, with some patients exhibiting a less severe course and longer survival times.<sup>2,3</sup> Clinically, fasciculation and an increase in muscular weakness are linked to motor neuron loss. Patients suffer from paralysis in the final stages of the illness. Furthermore, minor memory loss and cognitive impairment may be present in up to 50% of individuals. The ultimate result of ALS is paralysis and an early death that is typically brought on by respiratory failure.<sup>4–6</sup>

Degeneration of motor neurons in the spinal anterior horn and motor cortex, as well as axon loss in the lateral columns of the spinal cord, are the neuropathological characteristics of this neuromuscular disease.<sup>7</sup>

ALS is classified in two types: the familiar form (fALS) is the less frequent type of ALS and comprises approximately 5–10% of cases and the sporadic form (sALS) that represents the most common cause of ALS.<sup>8,9</sup>

The neuroinflammatory component of ALS is being characterized and includes the overexpression of mediators such as iNOS and TNF- $\alpha$ . Furthermore, complement involvement, macrophages and lymphocyte infiltration, microglia activation, and reactive astrocytes have been associated with this condition.<sup>10</sup>

Currently, there are no effective treatments for ALS. Indeed, riluzole, a NMDA glutamate receptor blocker, and edaravone, a ROS scavenger, are currently the sole two medications approved for ALS treatment. However, their efficacy in extending life expectancy typically amounts only few months.<sup>11</sup>

Indole scaffolds are the most common moiety in bicyclic heterocyclic structures present in natural and synthetic biologically relevant compounds. The indole group may be found in neurotransmitters and autacoids such as serotonin, melatonin, and melatonin, derived from the amino acid tryptophan, and in several alkaloids. Numerous synthetic methods have been elaborated to obtain thousands of small molecules based on the indole scaffold,<sup>12,13</sup> and almost 500 indole-based compounds are listed in DrugBank.<sup>14</sup>

Over the years, indole has proved to be a useful scaffold for the design of compounds provided with anti-inflammatory properties such as indomethacin, acetaminophen, and etodolac. Additionally, indomethacin has been previously demonstrated to be efficacious in different experimental models of neuroinflammation.<sup>15–17</sup>

Aiming to develop novel medicaments for the treatment of this neurodegenerative disease, two 2-methyl-3-indolylacetic derivatives, hereinafter identified as compounds II and III (Figure 1), already described as analgesic and anti-inflammatory compounds,<sup>18</sup> were selected and evaluated for their potential capability of slowing down neurodegeneration

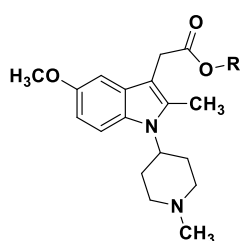


**Figure 1.** Chemical structures of compound II ( $R = H$ ) and compound III ( $R = CH_2CH_3$ ).

associated with ALS progression preclinical models in vitro and in vivo.

The analgesic activities were comparable to indomethacin, while notably neither of the compounds exhibited any gastric effects (gastric damage evaluated as the lengths of the lesions in millimeters; <sup>15</sup> indomethacin  $50 \pm 8$  mm vs compound III  $3 \pm 0.6$  mm and compound II 0 mm).

Additionally, compound IV was synthesized as a molecular hybrid of compound II with 4-hydroxythiobenzamide (Figure 2).

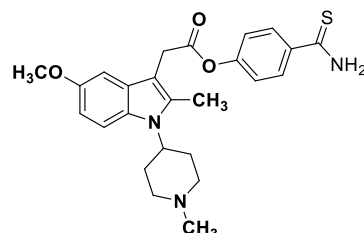


**Figure 2.** Chemical structure of compound IV.

The design of these molecules was done with the attempt of reducing the release of proinflammatory factors in the CNS. Neuroinflammation represents a crucial neurodegenerative mechanism; in fact, over the years, several findings associated this process to many neurodegenerative diseases, including multiple sclerosis (MS), Alzheimer's disease (AD), Parkinson's disease (PD), and amyotrophic lateral sclerosis. For this reason, several therapeutic interventions have been proposed with the aim of slowing down or blocking inflammation progression occurring in neurodegenerative diseases, with particular emphasis given to the role of TNF- $\alpha$ .<sup>19–23</sup>

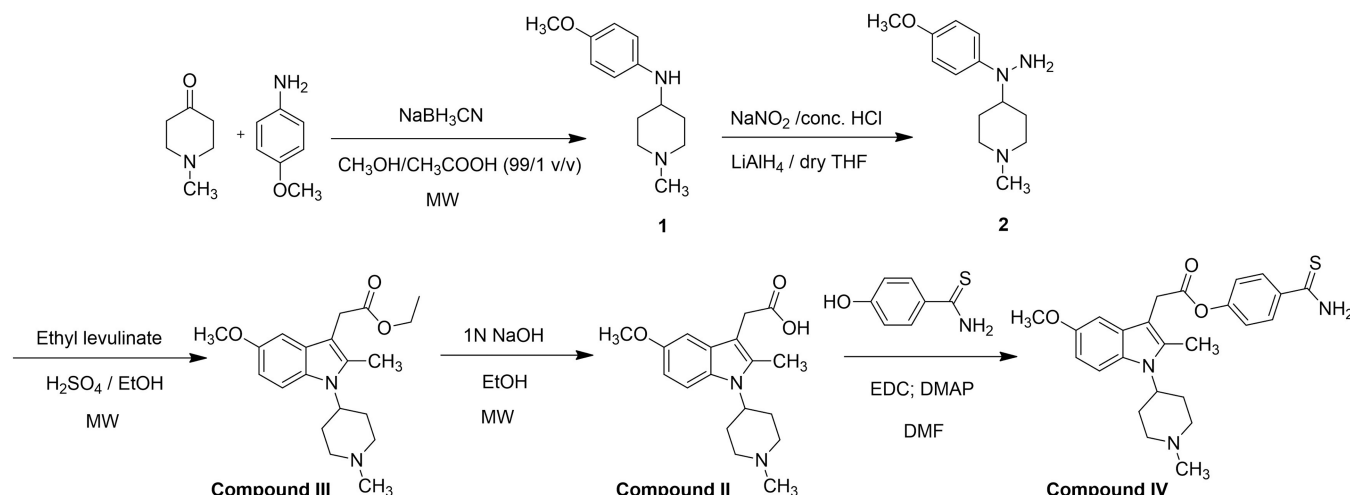
## 2. MATERIAL AND METHODS

All of the commercial reagents and solvents have been purchased from Merck-Sigma-Aldrich. Utilizing a Heidolph MR Hei-Standard magnetic stirrer, reactions were agitated at 400 rpm. A Buchi R-114 rotary evaporator was used to concentrate the solutions under low pressure. Using Merck silica gel 60 F254 plates that had a fluorescent indicator applied and UV light (254 nm) to visualize the reactions, TLC was used to monitor each reaction. A silica gel column (Kieselgel 60) was used for preparatory chromatographic purifications.

Utilizing a microwave oven (ETHOS 1600, Milestone) specifically developed for organic synthesis, microwave reactions were carried out. A preliminary analysis was done to determine the ideal profile power/time and temperature for the synthesis. An embedded fluoroptic probe that was microwave-transparent was used to directly measure the temperature of the agitated reaction mixture.

The uncorrected melting points were obtained with a Buchi Melting Point B-540 device. Final product mass spectra were obtained using an LTQ Orbitrap XLT™ Fourier transform mass spectrometer (FTMS) fitted with a positive mode-operating ESI ION MAX™ (Thermo Fisher, San José, CA, USA) source. Utilizing a Varian Mercury Plus 600 MHz device, we recorded NMR studies. Every spectrum was captured in  $DMSO-d_6$ . Chemical shifts are indicated in ppm. When applicable, the abbreviations s (singlet), d (doublet), dd (double doublet), q (quartet), and m (multiplet) are used to indicate peak patterns.

Scheme 1. Synthetic Route for Compounds II–IV



**2.1. Chemistry.** For the preparation of compounds II–IV, we followed with modifications the procedures adopted in the literature.<sup>21</sup> The synthetic route is reported in Scheme 1. Microwave irradiation proved to increase the yields and reduce the reaction times for the preparation of intermediates 1, compound III and II. Briefly, a reductive amination of *p*-anisidine with 1-methylpiperidin-4-one in the presence of sodium cyanoborohydride in CH<sub>3</sub>OH containing 1% of acetic acid by microwave irradiation was carried out to obtain the aniline derivative 1. The hydrazine 2 was obtained via nitrosation and subsequent reduction with LiAlH<sub>4</sub> of the resulting nitro group. Afterward, compound III was prepared by the Fischer indole synthesis, using a single acid catalyst in “one-pot” conversion by flash microwave irradiation yielding compound III in very high yield 92% and short irradiation time (55') (Scheme 1). Starting from compound III, compound II was obtained by ethyl ester saponification. Coupling of this latter with 4-OH-thiobenzamide by EDC gave the desired ester corresponding to compound IV.

**2.1.1. *N*-(1-Methyl-4-piperidinyl)-4-anisidine (1).** *p*-Anisidine (10 g, 0.081 mol) and 1-methylpiperidin-4-one (7.1 g, 0.063 mol) were dissolved in a CH<sub>3</sub>OH/CH<sub>3</sub>COOH mixture (60 mL, 99:1, v/v) and were stirred at room temperature for 10 min. NaBH<sub>3</sub>CN (2.58 g, 0.041 mol) was dissolved in methanol (10 mL), and once added to the reaction, the mixture was heated by microwave (1 h, 45 °C, 300W). The solvent was removed by evaporation, and the crude substance was then dissolved in 350 mL of ethyl acetate. Three 50 mL portions of brine and 50 mL of water were used to wash it. Na<sub>2</sub>SO<sub>4</sub> anhydrous was used to dry the organic layer, and the solvent was then evaporated once more. After chromatography with a 6:4 dichloromethane/methanol eluent on a silica gel column, 13.04 g of compound 1 was obtained as an oil in a yield of 95%.

**2.1.2. *N*-(1-Methyl-4-piperidinyl)-4-anisylhydrazine (2).** *N*-(1-Methyl-4-piperidinyl)-4-anisidine (1, 6.5 g, 0.03 mol) in 70 mL of absolute ethanol was cooled to 0 °C and stirred. Slowly, 63.3 mL of 37% HCl was added. A solution of NaNO<sub>2</sub> (2.64 g, 0.04 mol) in 15 mL of water was then added dropwise, maintaining the temperature below 0 °C. The mixture was stirred at 0 °C for an additional 3 h. Then, 200 mL of water was added, and the mixture was treated with 6N NaOH until it became alkaline. The solution was extracted with ethyl acetate

(3 × 200 mL), washed with water, dried over anhydrous Na<sub>2</sub>SO<sub>4</sub>, and filtered, and the solvent was removed. The resulting crude nitroso compound was utilized without additional purification. It was dissolved in THF and added dropwise to a suspension of LiAlH<sub>4</sub> (3.2 g) in 28 mL of THF. The mixture was stirred at reflux for 1 h and then allowed to cool to room temperature. Subsequently, 10 mL of water and 10 mL of 3N NaOH were added dropwise. The mixture was filtered through Celite, and the residue was washed multiple times with dichloromethane. The solvent was evaporated, yielding 6.1 g of compound 2 (88%).

**2.1.3. Ethyl 2-(5-methoxy-2-methyl-1-(1-methylpiperidin-4-yl)-1*H*-indol-3-yl)acetate (Compound III).** *N*-(1-Methyl-4-piperidinyl)-4-anisylhydrazine 2 (4.7 g, 0.020 mol) and ethyl levulinate (2.88 g, 0.020 mol) were placed in a closed vessel, using 80 mL of absolute ethanol as the solvent. The mixture was heated using microwave irradiation at 78 °C, and the reaction was stirred for 40 min (400W). The residue was dissolved in absolute ethanol, treated with sulfuric acid (96%, 1 mL), and added in a closed vessel. The mixture was heated to 78 °C by microwave irradiation (400 W) for 15 min and then alkalinized by adding 1N NaOH solution.

After removing the ethanol by evaporation, ethyl acetate was added as a solvent and the extraction was performed three times (3 × 150 mL). The organic phases were washed with brine and then dried over anhydrous Na<sub>2</sub>SO<sub>4</sub> and filtered. Finally, the solvent was removed under vacuum and the crude product was purified by silica gel open chromatography using dichloromethane/methanol/NH<sub>4</sub>OH (94:5:1 v/v) as an eluent. Compound III (6.4 g) was obtained with a yield of 92% and a melting point of 68–70 °C.

<sup>1</sup>H NMR (600 MHz, DMSO-*d*<sub>6</sub>) δ 7.39 (d, 1H, *J* = 8.9 Hz), 6.93 (d, 1H, *J* = 2.1 Hz), 6.66 (dd, 1H, *J* = 8.9 Hz, 2.1 Hz), 4.16 (m, 1H), 4.06 (q, 2H, *J* = 6.9 Hz), 3.74 (s, 3H), 3.62 (s, 2H), 2.91 (m, 2H), 2.36 (m, 5H), 2.24 (s, 3H), 2.10 (m, 2H), 1.69 (m, 2H), 1.18 (t, 3H, *J* = 6.9 Hz).

<sup>13</sup>C NMR (150 MHz, DMSO-*d*<sub>6</sub>) δ 172.0, 153.4, 135.3, 129.9, 129.2, 112.1, 110.0, 104.1, 100.8, 60.4, 55.8, 55.6, 53.4, 46.4, 30.6, 30.5, 14.6, 11.5. ESI-MS: 345.2 [M + H]<sup>+</sup>.

**2.1.4. 2-(5-methoxy-2-methyl-1-(1-methylpiperidin-4-yl)-1*H*-indol-3-yl)acetic acid (Compound II).** Ethyl 2-(5-methoxy-2-methyl-1-(1-methylpiperidin-4-yl)-1*H*-indol-3-yl)acetate (III, 4 g, 0.011 mol) was placed in a closed vessel and

dissolved in 70 mL of ethanol. Then, a solution of 1 N NaOH (40 mL) was added. The mixture was heated to 78 °C by microwave irradiation for 3 min (500 W) and then neutralized with a solution of 1 N HCl.

After removal of the ethanol by evaporation, ethyl acetate was added as a solvent, and the extraction was performed three times (3 × 150 mL). The organic phases were washed with brine and then dried over anhydrous Na<sub>2</sub>SO<sub>4</sub> and filtered. Finally, the solvent was removed under vacuum, and compound II was obtained (3.4 g) with a yield of 98% and a melting point of 172–173 °C.

<sup>1</sup>H NMR (600 MHz, DMSO-*d*<sub>6</sub>) δ 7.49 (d, 1H, *J* = 8.9 Hz), 6.93 (d, 1H, *J* = 2.1 Hz), 6.66 (dd, 1H, *J* = 8.9 Hz, 2.1 Hz), 4.25 (m, 1H), 3.73 (s, 3H), 3.55 (s, 2H), 3.05 (m, 2H), 2.54 (m, 2H), 2.36 (m, 5H), 2.35 (s, 3H), 1.73 (m, 2H).

<sup>13</sup>C NMR (150 MHz, DMSO-*d*<sub>6</sub>) δ 173.8, 153.3, 135.0, 129.8, 129.4, 112.0, 109.8, 105.1, 101.1, 55.8, 55.2, 52.8, 45.8, 31.0, 30.0, 11.5. ESI-MS: 317.2 [M + H]<sup>+</sup>.

**2.1.5. 4-Carbamothioylphenyl-2-(5-methoxy-2-methyl-1-(1-methylpiperidin-4-yl)-1H-indol-3-yl)acetate (Compound IV).** [5-Methoxy-2-methyl-1-(1-methylpiperidin-4-yl)-1H-indol-3-yl]-acetic acid (II, 1 g, 0.00316 mol) was dissolved in dimethylformamide (10 mL); EDAC (0.67 g, 0.00340 mol) and DMAP (0.040 g, 0.000316 mol) were added, and the reaction mixture was kept under stirring for 10 min at a temperature of 0 °C. Then, 4-hydroxythiobenzamide (0.73 g, 0.00474 mol) was added to the mixture, and the reaction was kept under stirring at room temperature overnight. The solvent was removed by distillation under reduced pressure, and the residue was purified by silica gel column chromatography (dichloromethane/methanol, 8:2, v/v) giving 630 mg of compound IV. Yield 44%. Yellow solid. M.p.: 145–146 °C.

<sup>1</sup>H NMR (600 MHz, DMSO-*d*<sub>6</sub>) δ 9.90 (s, 1H), 9.52 (s, 1H), 7.93 (d, 2H, *J* = 8.6 Hz), 7.49 (d, 1H, *J* = 8.9 Hz), 7.14 (d, 2H, *J* = 8.6 Hz), 6.93 (d, 1H, *J* = 2.1 Hz), 6.73 (dd, 1H, *J* = 8.9 Hz, 2.1 Hz), 4.53 (m, 1H), 3.99 (s, 2H), 3.78 (s, 3H), 2.94 (m, 2H), 2.43 (s, 3H), 2.42 (m, 2H), 2.28 (s, 3H), 2.14 (m, 2H), 1.73 (m, 2H).

<sup>13</sup>C NMR (150 MHz, DMSO-*d*<sub>6</sub>) δ: 199.0, 170.2, 153.1, 152.8, 137.0, 135.2, 129.7, 128.8, 128.7, 121.2, 114.3, 109.7, 102.9, 100.4, 55.4, 55.1, 52.9, 45.9, 30.0, 29.9, 11.1. ESI-MS: 452.3 [M + H]<sup>+</sup>.

**2.2. Cell Lines.** Human neuroblastoma SH-SY5Y cell cultures (Cell bank Line Collection ICLC) and immortalized murine microglial BV-2 cell lines were grown as monolayers in polystyrene dishes (12 or 6 wells plate) in Dulbecco's modified Eagle's medium (DMEM) with 10% (v/v) fetal bovine serum (FBS), L-glutamine (2 mM), 1% penicillin (50 IU/mL), and streptomycin (50 µg/mL). Cells were grown in a humidified atmosphere containing 95% air and 5% CO<sub>2</sub>, and the medium was changed every 2 days. All experiments were conducted in cultures containing cells between the fourth and eighth passages.

SH-SY5Y and BV-2 cells were plated with a confluence of 65,000 cell/mL. After 24 h of cell seeding, medium was changed for 6 h starvation in a medium without FBS.

In order to reproduce in vitro some of the ALS features, the cyanobacterial toxin  $\beta$ -N-methylamino-L-alanine (L-BMAA) at 2 mM for 120 h in a medium without FBS was used on SH-SY5Y cells, as previously reported.<sup>24–32</sup> The neurotoxin was replaced after 1, 3, or 5 days while indolylacetic derivatives II, III, and IV (1,10, 100 nM and 1 µM) were added 20 min before each L-BMAA treatment to the medium.

BV-2 cells were exposed to bacterial toxin lipopolysaccharides (LPS) at 100 ng/mL and indolylacetic derivatives II, III, and IV (100 nM) for 24 h in a medium without FBS.

Cells were exposed to compounds or vehicle (control, ct), medium without FBS) and, after 24 h, were analyzed for Western blotting experiments or MTT assay.

### 2.3. Determination of Cell Viability and Nitric Oxide

**Production.** Cell viability was revealed as previously described<sup>24</sup> by using the MTT (Sigma-Aldrich, Milan Italy) staining.

In particular, the media was removed from the cells after 24 h of treatment, the cells were then incubated for 1 h at 37 °C in 0.5 mg/mL of MTT solution. Acidified isopropanol (500 µL) was added to halt the incubation and dissolve the formazan salt. A spectrophotometer was used to measure the absorbance at 540 nm to determine the viability.

Using the Griess method, nitrite was evaluated to determine the amount of nitric oxide (NO) produced in supernatants.<sup>25</sup> The media was reacted with the same volume of Griess reagent (0.1% *N*-1-naphthylenediamine dihydrochloride and 1% sulfanilamide in 1% phosphoric acid) for 10 min, and absorbance at 540 nm was measured by a spectrophotometer (SpectraMax iDS). Background correction was achieved using the same cell culture medium as blank.

**2.4. Western Blot Analysis.** Western blot analysis was performed as previously described.<sup>24</sup> Protein samples (50 µg) were analyzed on 8% SDS-polyacrylamide gel subjected to electrophoresis (SDS-PAGE) and electrotransferred onto Hybond ECL nitrocellulose paper (Amersham, Milan, Italy). Membranes were blocked with 3% BSA in 0.1% Tween-20 (TBS-T; 2 mM Tris-HCl, 50 mM NaCl, pH 7.5) for 1 h at RT and subsequently incubated overnight at 4 °C in the blocked buffer with antibodies against iNOS (Rabbit monoclonal 1:1000 dilution; abcam), COX2 (Rabbit polyclonal 1:1000 dilution, byorbyt), TNF- $\alpha$  (Rabbit polyclonal 1:1000 dilution, Cell Signaling), and  $\beta$ -Actin (Mouse monoclonal, 1:10000, Sigma-Aldrich). Tween 20 (0.1%) was used to wash membranes that were then incubated with the secondary antibodies at room temperature for 1 h (1:1000; Amersham, Milan, Italy).

Immunoreactive bands were detected using an ECL (Amersham). Chemi-Doc Imaging System (Bio-Rad, Segrate, Italy) was used to determine the optical density of the bands (normalized for  $\beta$ -actin).

**2.5. Animal Model.** Tests were carried out on mice B6SJLTgN(SOD1G93A)1Gur overexpressing human SOD1, containing the Gly93Ala mutation (The Jackson Laboratory, stock number 002726). They were identified by PCR genotyping according to protocol provided by The Jackson Laboratory's.<sup>26</sup>

In total, 24 male and female mice maintained in rooms with 12 h darkness and light cycles were used. Every experimental group included an equal number of male and female mice (12 vs 12).

According to international criteria for animal research, experiments, which included chemical administrations and behavioral tests, were conducted between 12 and 4 p.m. and were approved by the Ministry of Health, Italy (759/2019-PR) and the Animal Care Committee of Federico II University of Naples, Italy. Every attempt was made to lessen the amount of pain experienced by animals and to use fewer animals overall.

**2.6. In Vivo Treatment.** The compound III, dissolved in 0.9% (isotonic) saline, was intraperitoneally administered (1

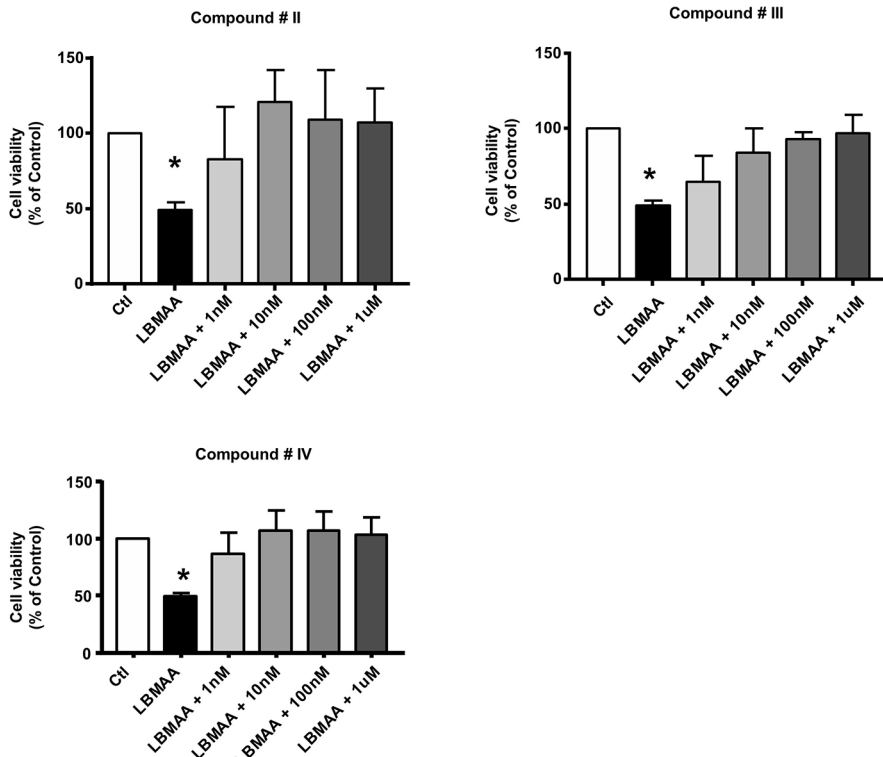


**Figure 3.** Survival of SHSY-5Y cells exposed to L-BMAA neurotoxin induced by compounds II, III, and IV. The MTT assay was performed 24 h after the last exposure to compounds and L-BMAA. Compounds II, III, and IV were added 20 min before each L-BMAA-exposure. Each data point is the mean  $\pm$  SEM. One-way ANOVA followed by Bonferroni's multiple comparison test was used for statistical analysis.  $n =$  at least 3 for group. \* $p < 0.05$  versus control.

$\mu$ L) everyday at a dose of 1 or 10 mg/kg, starting at 2 months of age up until 4.5 months of age.

**2.6.1. Evaluation of Motor Performance.** Behavioral tests were performed once per week. For the hind limb test, the mouse was positioned on a grid (45 cm long  $\times$  28 cm large). The lid was lightly shaken to allow the animal to hold onto the grid, before it was quickly turned upside down. The amount of time that the mouse was able to stay on the grid was used to calculate its grip score. Cut-off time was arbitrary set at 90 s.<sup>26</sup>

A five-station mouse rotarod apparatus was used to evaluate balance and motor coordination (Ugo Basile; Milan, Italy).<sup>26</sup> The rod measured 6 cm in length and 3 cm in diameter at each site. The mice were trained to keep their balance while being sped up to a steady speed of 14 rpm for three trials in a row. A single rotarod trial, given once a week, was used to administer the tests. For a time interval of 180 s, the rotational speed was increased from 4 to 14 rpm. The latencies to fall of the mice were assessed once a week and then averaged after they completed three trials on the rotarod. The mice that did not fall at all were given a maximum delay of 180 s. The paralysis of the rear limbs was assessed every week. The animal was scored for having paralyzed hind limbs when it was dragged by one of its hind limbs. When the mouse was unable to utilize its forelimbs to walk or turn itself around, it was assessed as having paralysis of that limb. The weight of the mouse was taken at the right before each behavioral test session.

When mice were placed on their sides and could not correct themselves after 20 s, it was considered the final stage of the disease.

**2.7. Statistical Analysis.** The data was assessed using means  $\pm$  SEM. One-way ANOVA was used to identify

statistically significant differences between means, and for Western blotting, the Student–Newman–Keuls/Bonferroni posthoc test was used to confirm the results.

Behavioral test (grip and rotarod) results were analyzed by two-way ANOVA followed by the posthoc test. Utilizing the Kaplan–Meier plot, survival was assessed. The student's *t* test was employed to compare the two groups. At the 95% confidence level, statistical significance was deemed acceptable ( $p < 0.05$ ). In order to conduct statistical analysis, GraphPad Prism 5.0 (La Jolla, CA, USA) was used. Every experiment was conducted in a blinded manner.

### 3. RESULTS AND DISCUSSION

**3.1. Indolylacetic Derivatives Enhanced the Survival of Neuronal Cells Exposed to L-BMAA and Reduced Neuroinflammation.** To test whether indolylacetic derivatives protect against L-BMAA-induced toxicity, human SH-SY5Y neuroblastoma cell cultures were treated with L-BMAA and compounds II–IV. MTT assay, used to quantify cell survival, was carried out in (1) vehicle exposed cells (control, Ctl), (2) L-BMAA exposed cells, and (3) cells exposed to L-BMAA and different concentrations of the newly synthesized compounds II–IV (1, 10, and 100 nM and 1  $\mu$ M). Surprisingly, all derivatives were able to rescue the toxic effect induced by L-BMAA exposure (Figure 3).

Indolylacetic derivatives II–IV enhanced the survival of neuronal cells exposed to L-BMAA. Furthermore, Western blotting with the inflammation markers COX<sub>2</sub>, iNOS, and TNF- $\alpha$  antibodies revealed that compounds II and IV were able to prevent iNOS elevation in microglial BV2 cells elicited by LPS (Figure 4), unlike compound III, which did not even

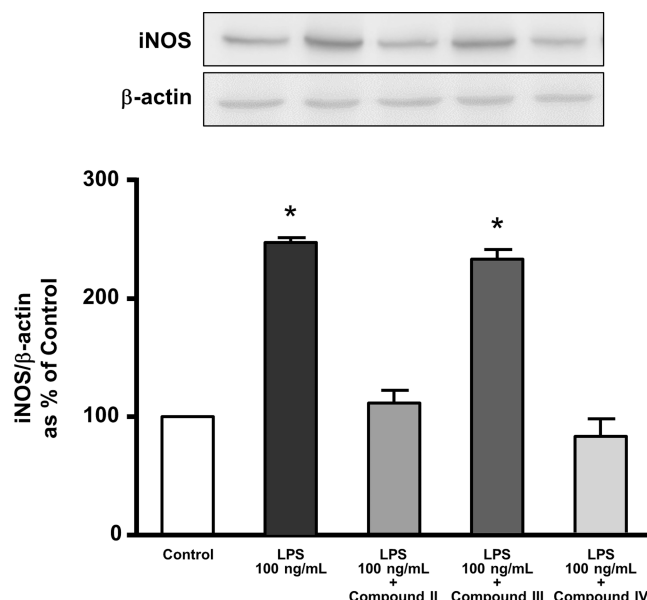


**Figure 4.** Effects of compounds II–IV on iNOS expression induced by LPS exposure in microglia cell cultures. Representative Western blots and densitometric quantification of iNOS levels in BV-2 microglial cell cultures. Data were normalized on the  $\beta$ -actin levels.  $n$  = at least 3 for column. Each data point is the mean  $\pm$  SEM. One-way ANOVA followed by Bonferroni's multiple comparison test was used for statistical analysis. \* $p$  < 0.05 versus control.

attenuate the production of nitric oxide (Figure 5). By contrast, compound III was able to prevent the overexpression

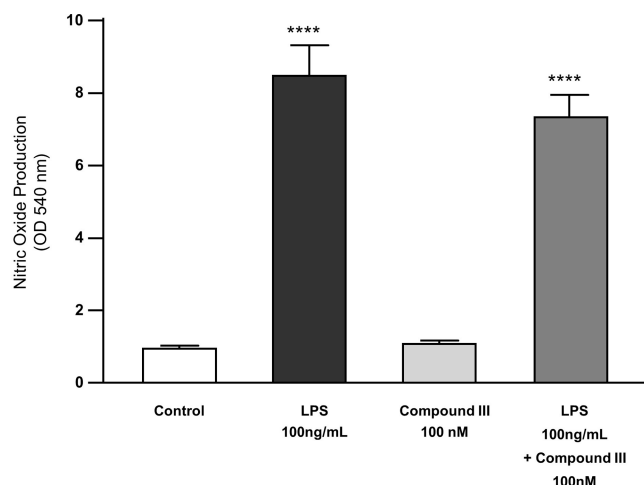


**Figure 5.** Effect of compound III on NO generation induced by LPS in BV-2 microglia cell cultures. Each data point is the mean  $\pm$  SEM. One-way ANOVA followed by Bonferroni's multiple comparison test was used for statistical analysis.  $n$  = at least 3 for column. \*\*\*\* $p$  < 0.0001 vs control group.

of TNF- $\alpha$  induced by LPS exposure (Figure 6). All considered compounds did not modify the COX<sub>2</sub> expression (Figure 7). Notably, reactive astrocytes and microglia in the central nervous system (CNS) may release TNF- $\alpha$ , one of the primary mediators of the inflammatory response. Indeed, elevated TNF- $\alpha$  has been reported in CNS tissue, serum, cerebrospinal fluid, and plasma from ALS patients as well as transgenic animal models of the disease.

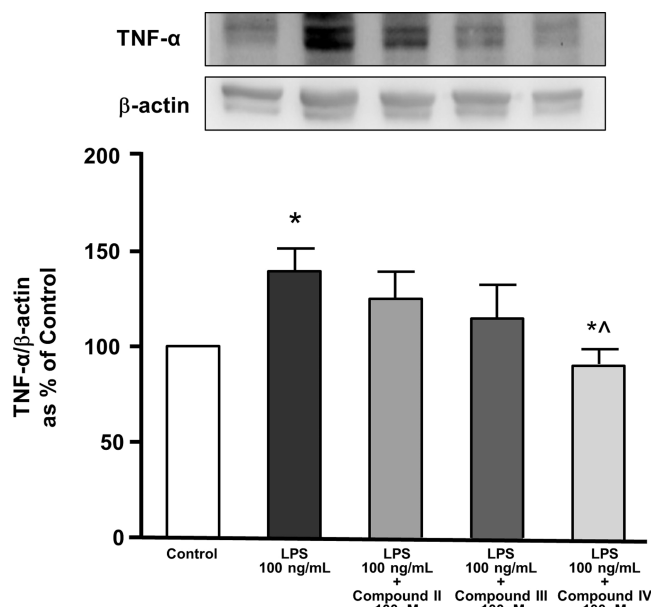


**Figure 6.** Effects of compounds II–IV on LPS-induced TNF- $\alpha$  expression in microglia cells. Representative Western blot and densitometric quantification of TNF- $\alpha$  in BV-2 microglial cells. Data were normalized on the  $\beta$ -actin levels.  $n$  = at least 3 for column. Each data point is the mean  $\pm$  SEM. One-way ANOVA followed by Bonferroni's multiple comparison test was used for statistical analysis. \* $p$  < 0.05 versus control;  $^p$  < 0.05 versus LPS 100 ng/mL.

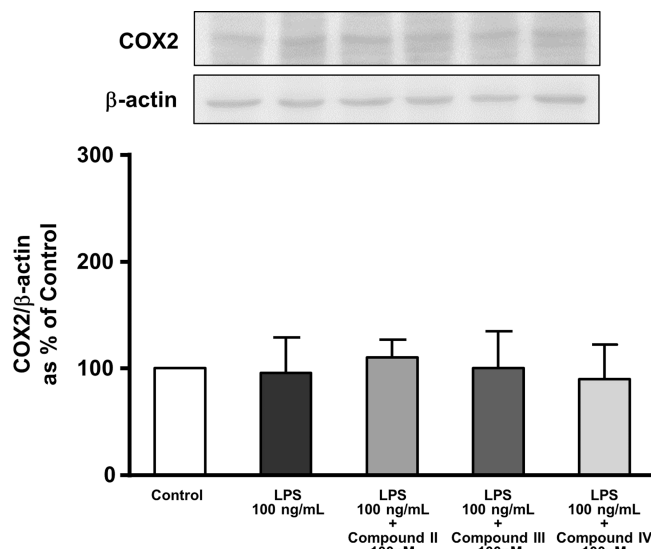


**Figure 7.** Effects of compounds II–IV on LPS-induced COX2 expression in microglia cells. Representative Western blot and densitometric quantification of COX2 in BV-2 microglial cells. Data were normalized on the  $\beta$ -actin levels.  $n$  = at least 3 for column. Each data point is the mean  $\pm$  SEM. One-way ANOVA followed by Bonferroni's multiple comparison test was used for statistical analysis.

**3.2. Prolonged Compound III Treatment of SOD1 G93A Mice Reduced Motor Symptoms and Improved Survival Rate.** Behavioral tests were conducted on WT and SOD1 G93A mice on a weekly basis beginning from the second month after birth (P60), when ip administration of compound III commenced and the mice were asymptomatic, to determine whether the reduced neuroinflammatory response seen in vitro through the effect on TNF- $\alpha$  expression

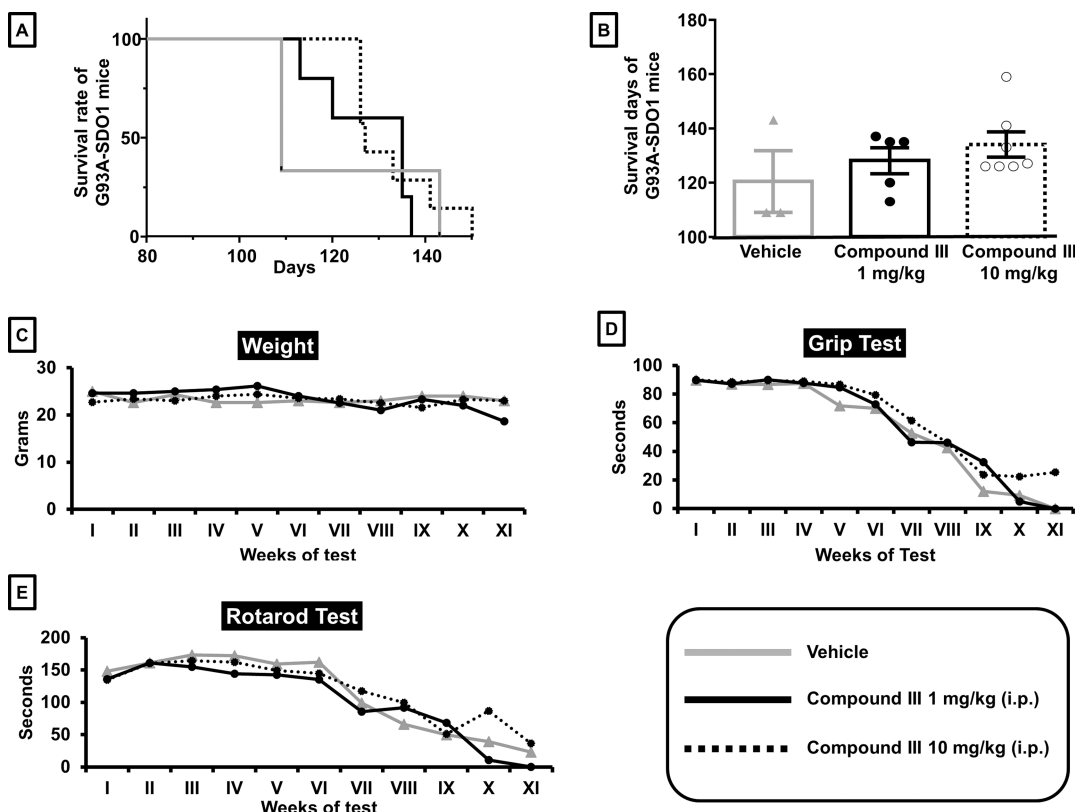


**Figure 8.** Effect of prolonged compound III treatment on motor symptoms and survival rates in ALS-affected mice (SOD1 G93A).

was accompanied by an improvement of these mice's motor performance. Mice were divided into three experimental groups: SOD1 G93A+vehicle, SOD1 G93A + compound III at 1 mg/kg, and SOD1 G93A + compound III at 10 mg/kg, then weighed, and subjected to rotarod and grip tests.

**3.2.1. Survival.** Compound III at the higher dose considered prolonged the ALS mice survival rate (Figure 8A). Indeed, the lifespan of vehicle-treated SOD1 G93A mice was  $95 \pm 13$  days, while that of ALS mice treated with compound III at the dose of 1 mg/kg was  $128.0 \pm 4.8$  days and that of ALS mice treated with compound III at the dose of 10 mg/kg was significantly longer, being  $134.0 \pm 4.7$  days (Figure 8B).

When denervation-induced muscle atrophy produced 15–20% of the reduction in motor performance, including grip strength and rotarod performance, it was considered to be the start of the disease. In fact, the paralysis onset was  $33.69 \pm 1.31$  days for the SOD1G93A group treated with vehicle and  $42.47 \pm 1.59$  days for the compound III-treated SOD1G93A group.

**3.2.2. Body Weight.** Body weight loss is usually detected quite late in vehicle-treated SOD1 G93A mice. Indeed, in all group SOD1 G93A treated with both vehicle or compound III for 10 weeks, the weight remained stable over time (Figure 8C).

**3.2.3. Grip-Strength Test.** The hindlimb grip test was carried out by placing the mouse upside-down on a grid and evaluating the latency to fall off the grid up to a maximum of 90 s. After 5 weeks of therapy, the loss of limb strength became apparent in the vehicle-treated SOD1 G93A mice (ALS+vehicle:  $71.9 \pm 25.8$  s). However, in ALS mice treated with compound III, the grip performance was slightly but not significantly improved from the fifth week of treatment (ALS+1 mg/kg:  $84.8 \pm 11.6$  s; ALS+10 mg/kg:  $86.9 \pm 5.5$  s), in particular with the higher dosage of compound III (Figure 8D).

8D). The best results were observed with compound III 10 mg/kg at the tenth and eleventh week of treatment (Figure 8D).

**3.2.4. Rotarod Test.** The ability of G93A mice to maintain balance on an accelerating rotarod during the course of the 10-week treatment was used to measure the mice's motor coordination. Typically, the first 2 weeks of behavioral testing are regarded as the training phase. Therefore, a progressive impairment of motor coordination in G93A mice became evident at the age of 3 months approximatively, at fifth week after treatment beginning. Unfortunately, there were no overall statistically significant differences between G93A treatment groups. A significant improvement in rotarod performance was observed in G93A mice treated with 10 mg/kg of compound III at the seventh week of treatment (VII: ALS+vehicle:  $99.1 \pm 61$  s; ALS+10 mg/kg:  $117.4 \pm 32.7$  s). A slightly but not significant improvement in motor performances was observed also after 8 and 10 weeks of treatment (Figure 8E).

## 4. CONCLUSIONS

In the current manuscript, we provided evidence that the newly synthesized 2-methyl-3-indolylacetic derivatives: (1) prevented the upregulation of TNF- $\alpha$  observed in BV-2 microglial cells exposed to the toxin LPS, (2) preserved SHSY-5Y cell survival exposed to L-BMAA neurotoxin, and (3) enhanced survival rate and alleviated motor signs of SOD1G93A ALS mice.

Currently, ALS represents a medical need since only few, nonresolutive treatments are available for this debilitating neurodegenerative condition, which progresses and results in the death of motor neurons in the brainstem, spinal cord, and motor cortex.<sup>11</sup>

The ALS neuroinflammatory component is being characterized, and different from the canonical knowledge in the field attribute to COX activity the main player of this process, it includes the overexpression and activation of molecular pathways involving the tumor necrosis factor- $\alpha$ .<sup>20–23</sup> TNF- $\alpha$  is a cytokine that plays a role in many physiological and pathological processes. These processes include cell proliferation, cell death, and inflammation.<sup>20–23</sup> In the context of ALS, TNF- $\alpha$  has been implicated in the neuroinflammatory processes that contribute to the progression of the disease.<sup>20–23</sup>

Several studies have suggested that compared to healthy subjects, TNF- $\alpha$  levels are increased in the CNS of people affected by ALS. This increase is thought to be associated with the activation of microglia and astrocytes, leading to neuroinflammation and subsequent neuronal damage. TNF- $\alpha$  can induce the generation of further proinflammatory cytokines and promote inflammatory pathways, further exacerbating neuroinflammation in ALS.<sup>20–23</sup> Furthermore, TNF- $\alpha$  has been linked to neurotoxicity and neuronal death. It can trigger apoptotic pathways and contribute to excitotoxicity, leading to the degeneration of motor neurons.<sup>20–23</sup>

However, the role of TNF- $\alpha$  in ALS is intricate and not completely understood. Some findings indicate that TNF- $\alpha$  may be not directly involved in SOD1-related ALS.<sup>35</sup>

Overall, it is possible to hypothesize that TNF- $\alpha$  likely plays a different role in different ALS phenotypes/genotypes, contributing to both neuroinflammation and neurotoxicity. Targeting TNF- $\alpha$  and its downstream pathways may hold therapeutic potential for ALS treatment.

Based on that reported above, we have developed novel 2-methyl-3-indolylacetic derivatives able to prevent ALS-induced TNF- $\alpha$  upregulation. These compounds have been then evaluated for their potential capability of slowing down neurodegeneration associated with ALS progression in preclinical in vitro and in vivo ALS models.

The synthesized compounds II–IV showed that a significant effect in the control of cell death induced in vitro by the exposure of SH-SY5Y neuronal cell lines to the neurotoxin L-BMAA. In fact, we and others demonstrated that a form of ALS/Parkinson's dementia phenotypically similar to familial forms of ALS can be induced by the exposure to the L-BMAA toxin.<sup>24–32</sup> It has indeed been demonstrated that exposure to L-BMAA can induce endoplasmic reticulum stress, accumulation of misfolded proteins, and alterations in intracellular calcium concentrations.<sup>29–31</sup> Furthermore, our research group recently demonstrated that chronic intraperitoneal administration of 30 mg/kg for 30 days in Wt mice was able to reproduce motor and cognitive impairments. Moreover, it was able to induce the accumulation of the TDP43 protein in the cytosol of cells exposed to L-BMAA, reproducing the form of ALS frontotemporal dementia. Therefore, we believe that for the objectives of the current study, the model of L-BMAA appears to be adequate to reproduce in vitro some toxicity mechanisms related to ALS.<sup>32</sup>

As for the mechanism of action, compounds II and IV were able to prevent iNOS expression induced in BV2 microglial cells by LPS exposure. Compound III was able to prevent TNF- $\alpha$  expression but not COX<sub>2</sub>, induced in BV2 microglial cells by LPS exposure. Furthermore, compound III did not interfere with NO production, thus avoiding possible damage to motor neurons recently attributed to high levels of NO.<sup>33,34</sup> The use of SHSY5Y cells to test the protective effect of the

newly synthesized compounds in vitro may represent a limitation of the study. However, in vitro studies were carried out on SHSY5Y cells for a rapid preliminary screening. The most promising compound, that is, compound III, has been then evaluated in vivo. Notably, compound III treatment increased the survival rate in ALS mice (SOD1 G93A), thus further supporting the neuroprotective effect of this class of compounds in ALS.

In conclusion, the results described herein support the potential of the synthesized indolylacetic derivatives II–IV in ALS treatment. Indeed, in the attempt to realize an association between two active molecules, we assumed that the combination of the indispensable moieties of two small molecules (the opioids containing a 4-piperidinyl ring with the FANS indomethacin) might lead to new medicaments potentially useful for the treatment of amyotrophic lateral sclerosis.

## ■ AUTHOR INFORMATION

### Corresponding Author

**Giuseppe Pignataro** — *Division of Pharmacology, Department of Neuroscience, Reproductive and Odontostomatological Sciences, School of Medicine, "Federico II" University of Naples, Naples 80131, Italy; [orcid.org/0000-0002-7290-4397](https://orcid.org/0000-0002-7290-4397); Phone: +39 081-7463332; Email: [giuseppe.pignataro@gmail.com](mailto:giuseppe.pignataro@gmail.com), [giuseppe.pignataro@unina.it](mailto:giuseppe.pignataro@unina.it)*

### Authors

**Angela Corvino** — *Department of Pharmacy, School of Medicine, "Federico II" University of Naples, Naples 80131, Italy*

**Giuseppe Caliendo** — *Department of Pharmacy, School of Medicine, "Federico II" University of Naples, Naples 80131, Italy*

**Ferdinando Fiorino** — *Department of Pharmacy, School of Medicine, "Federico II" University of Naples, Naples 80131, Italy; [orcid.org/0000-0001-7357-5751](https://orcid.org/0000-0001-7357-5751)*

**Francesco Frecentese** — *Department of Pharmacy, School of Medicine, "Federico II" University of Naples, Naples 80131, Italy; [orcid.org/0000-0001-8821-2937](https://orcid.org/0000-0001-8821-2937)*

**Valeria Valsecchi** — *Division of Pharmacology, Department of Neuroscience, Reproductive and Odontostomatological Sciences, School of Medicine, "Federico II" University of Naples, Naples 80131, Italy*

**Giovanna Lombardi** — *Division of Pharmacology, Department of Neuroscience, Reproductive and Odontostomatological Sciences, School of Medicine, "Federico II" University of Naples, Naples 80131, Italy*

**Serenella Anzilotti** — *Department of Science and Technology, University of Sannio, 82100 Benevento, Italy*

**Giorgia Andreozzi** — *Department of Pharmacy, School of Medicine, "Federico II" University of Naples, Naples 80131, Italy*

**Antonia Scognamiglio** — *Department of Pharmacy, School of Medicine, "Federico II" University of Naples, Naples 80131, Italy*

**Rosa Sparaco** — *Department of Pharmacy, School of Medicine, "Federico II" University of Naples, Naples 80131, Italy*

**Elisa Perissutti** — *Department of Pharmacy, School of Medicine, "Federico II" University of Naples, Naples 80131, Italy*

Beatrice Severino — Department of Pharmacy, School of Medicine, "Federico II" University of Naples, Naples 80131, Italy; [ORCID iD](https://orcid.org/0000-0002-3887-8869)

Michele Gargiulo — Miuli Pharma S.r.l., Nola 310 80035, Italy

Vincenzo Santagada — Department of Pharmacy, School of Medicine, "Federico II" University of Naples, Naples 80131, Italy

Complete contact information is available at:  
<https://pubs.acs.org/10.1021/acsphtsci.4c00098>

## Funding

This research was partially founded by Miuli Pharma S.r.l.

## Notes

The authors declare no competing financial interest.

## ■ REFERENCES

- (1) Tokuda, E.; Furukawa, Y. Copper Homeostasis as a Therapeutic Target in Amyotrophic Lateral Sclerosis with SOD1Mutations. *Int. J. Mol. Sci.* **2016**, *17* (5), 636.
- (2) Hilton, J. B.; White, A. R.; Crouch, P. J. Metal-deficient SOD1 in amyotrophic lateral sclerosis. *J. Mol. Med.* **2015**, *93*, 481–487.
- (3) Brooks, B. R.; Miller, R. G.; Swash, M.; Munsat, T. L. El Escorial revisited: revised criteria for the diagnosis of amyotrophic lateral sclerosis. *Amyotroph. Lateral Scler. Other Motor Neuron Disord.* **2000**, *1*, 293–299.
- (4) Lomen-Hoerth, C.; Murphy, J.; Langmore, S.; Kramer, J. H.; Olney, R. K.; Miller, B. Are amyotrophic lateral sclerosis patients cognitively normal? *Neurology.* **2003**, *60* (7), 1094–1097.
- (5) Rusina, R.; Ridzon, P.; Kulist'ák, P.; Keller, O.; Bartos, A.; Buncová, M.; Fialová, L.; Koukolík, F.; Matěj, R. Relationship between ALS and the degree of cognitive impairment, markers of neurodegeneration and predictors for poor outcome. A prospective study. *Eur. J. Neurol.* **2020**, *17*, 23–30.
- (6) Ringholz, G. M.; Appel, S. H.; Bradshaw, M.; Cooke, N. A.; Mosnik, D. M.; Schulz, P. E. Prevalence and patterns of cognitive impairment in sporadic ALS. *Neurology.* **2005**, *65*, 586–590.
- (7) Saberi, S.; Stauffer, J. E.; Schulte, D. J.; Ravits, J. Neuropathology of amyotrophic lateral sclerosis and its variants. *Neurol. Clin.* **2015**, *33*, 855–876.
- (8) Wen, X.; Westergard, T.; Pasinelli, P.; Trott, D. Pathogenic determinants and mechanisms of ALS/FTD linked to hexanucleotide repeat expansions in the C9orf72 gene. *Neurosci. Lett.* **2017**, *636*, 16–26.
- (9) Katsuno, M.; Tanaka, F.; Sobue, G. Perspectives on molecular targeted therapies and clinical trials for neurodegenerative diseases. *J. Neurol. Neurosurg. Psychiatry.* **2012**, *83*, 329–335.
- (10) Sirabella, R.; Valsecchi, V.; Anzilotti, S.; Cuomo, O.; Vinciguerra, A.; Cepparulo, P.; Brancaccio, P.; Guida, N.; Blondeau, N.; Canzoniero, L. M. T.; Franco, C.; Amoroso, S.; Annunziato, L.; Pignataro, G. Ionic Homeostasis Maintenance in ALS: Focus on New Therapeutic Targets. *Front. Neurosci.* **2018**, *12*, 510.
- (11) Jaiswal, M. K. Calcium, mitochondria, and the pathogenesis of ALS: the good, the bad, and the ugly. *Front. Cell. Neurosci.* **2013**, *7*, 199.
- (12) Thanikachalam, P. V.; Maurya, R. K.; Garg, V.; Monga, V. An insight into the medicinal perspective of synthetic analogs of indole: A review. *Eur. J. Med. Chem.* **2019**, *180*, 562–612.
- (13) Kumari, A.; Singh, R. K. Medicinal chemistry of indole derivatives: Current to future therapeutic prospectives. *Bioorg. Chem.* **2019**, *89*, No. 103021.
- (14) Wishart, D. S.; Feunang, Y. D.; Guo, A. C.; Lo, E. J.; Marcu, A.; Grant, J. R.; Sajed, T.; Johnson, D.; Li, C.; Sayeeda, Z.; et al. DrugBank 5.0: A major update to the DrugBank database for 2018. *Nucleic Acids Res.* **2018**, *46*, D1074–D1082. update to the DrugBank database for 2018. *Nucleic Acids Res.* **2018**: *46*: D1074–D1082.
- (15) Monje, M. L.; Toda, H.; Palmer, T. D. Inflammatory blockade restores adult hippocampal neurogenesis. *Science.* **2003**, *302*, 1760–1765.
- (16) Netland, E. E.; Newton, J. L.; Majocha, R. E.; Tate, B. A. Indomethacin reverses the microglial response to amyloid beta-protein. *Neurobiol. Aging.* **1998**, *19*, 201–204.
- (17) Boehme, M.; Guenther, M.; Stahr, A.; Liebmann, M.; Jaenisch, N.; Witte, O. W.; Frahm, C. Impact of indomethacin on neuroinflammation and hippocampal neurogenesis in aged mice. *Neurosci. Lett.* **2014**, *572*, 7–12.
- (18) Perissutti, E.; Fiorino, F.; Renner, C.; Severino, B.; Roviezzo, F.; Sautebin, L.; Rossi, A.; Cirino, G.; Santagada, V.; Caliendo, G. Synthesis of 2-methyl-3-indolylacetic derivatives as anti-inflammatory agents that inhibit preferentially cyclooxygenase 1 without gastric damage. *J. Med. Chem.* **2006**, *49* (26), 7774–7780.
- (19) Amor, S.; Peferoen, L. A. N.; Vogel, D. Y. S.; Breur, M.; van der Valk, P.; Baker, D.; van Noort, J. M. Inflammation in neurodegenerative diseases - an update. *Immunology.* **2014**, *142* (2), 151–166.
- (20) Guidotti, G.; Scarlata, C.; Brambilla, L.; Rossi, D. Tumor Necrosis Factor Alpha in Amyotrophic Lateral Sclerosis: Friend or Foe? *Cells.* **2021**, *10* (3), 518. Mar 1 PMID: 33804386; PMCID: PMC8000008
- (21) Tortarolo, M.; Lo Coco, D.; Veglianese, P.; Vallarola, A.; Giordana, M. T.; Marcon, G.; Beghi, E.; Poloni, M.; Strong, M. J.; Iyer, A. M.; Aronica, E.; Bendotti, C. Amyotrophic Lateral Sclerosis, a Multisystem Pathology: Insights into the Role of TNF $\alpha$ . *Mediators Inflammation* **2017**, *2017*, 2985051. Epub 2017 Sep 10. PMID: 29081600; PMCID: PMC5610855
- (22) Thonhoff, J. R.; Simpson, E. P.; Appel, S. H. Neuroinflammatory mechanisms in amyotrophic lateral sclerosis pathogenesis. *Curr. Opin. Neurol.* **2018**, *31* (5), 635–639. PMID: 30048339
- (23) Jensen, B. K.; McAvoy, K. J.; Heinsinger, N. M.; Lepore, A. C.; Ilieva, H.; Haeusler, A. R.; Trott, D.; Pasinelli, P. Targeting TNF $\alpha$  produced by astrocytes expressing amyotrophic lateral sclerosis-linked mutant fused in sarcoma prevents neurodegeneration and motor dysfunction in mice. *Glia.* **2022**, *70* (7), 1426–1449. Epub 2022 Apr 26. PMID: 35474517; PMCID: PMC9540310
- (24) Laudati, G.; Mascolo, L.; Guida, N.; Sirabella, R.; Pizzorusso, V.; Bruzzaniti, S.; Serani, A.; Di Renzo, G.; Canzoniero, L. M. T.; Formisano, L. Resveratrol treatment reduces the vulnerability of SH-SY5Y cells and cortical neurons overexpressing SOD1-G93A to Thimerosal toxicity through SIRT1/DREAM/PDYN pathway. *Neurotoxicology.* **2019**, *71*, 6–15.
- (25) Cho, N.; Moon, E. H.; Kim, H. W.; Hong, J.; Beutler, J. A.; Sung, S. H. Inhibition of Nitric Oxide Production in BV-2 Microglial Cells by Triterpenes from *Tetrapanax papyriferus*. *Molecules.* **2016**, *21*, 459.
- (26) Anzilotti, S.; Brancaccio, P.; Simeone, G.; Valsecchi, V.; Vinciguerra, A.; Secondo, A.; Petrozziello, T.; Guida, N.; Sirabella, R.; Cuomo, O.; Cepparulo, P.; Herchuelz, A.; Amoroso, S.; Di Renzo, G.; Annunziato, L.; Pignataro, G. Preconditioning, induced by sub-toxic dose of the neurotoxin L-BMAA, delays ALS progression in mice and prevents Na $^{+}$ /Ca $^{2+}$  exchanger 3 downregulation. *Cell Death Dis.* **2018**, *9* (2), 206.
- (27) Arnold, F. J.; Burns, M.; Chiu, Y.; Carvalho, J.; Nguyen, A. D.; Ralph, P. C.; La Spada, A. R.; Bennett, C. L. Chronic BMAA exposure combined with TDP-43 mutation elicits motor neuron dysfunction phenotypes in mice. *Neurobiol. Aging.* **2023**, *126*, 44–57. Epub 2023 Feb 23. PMID: 36931113
- (28) Dias, F. R. P.; de Souza Almeida, R. R.; Sovrani, V.; Thomaz, N. K.; Gonçalves, C. A.; Quincozes-Santos, A.; Bobermin, L. D. Glioprotective Effects of Resveratrol Against BMAA-Induced Astroglial Dysfunctions. *Neurotox. Res.* **2022**, *40* (2), 530–541. Epub 2022 Mar 23. PMID: 35320508
- (29) Yin, H. Z.; Yu, S.; Hsu, C. I.; Liu, J.; Acab, A.; Wu, R.; Tao, A.; Chiang, B. J.; Weiss, J. H. Intrathecal infusion of BMAA induces selective motor neuron damage and astrogliosis in the ventral horn of

the spinal cord. *Exp. Neurol.* **2014**, *261*, 1–9. Epub 2014 Jun 8.

PMID: 24918341; PMCID: PMC4194249

(30) Petrozziello, T.; Boscia, F.; Tedeschi, V.; Pannaccione, A.; de Rosa, V.; Corvino, A.; Severino, B.; Annunziato, L.; Secondo, A.  $\text{Na}^+/\text{Ca}^{2+}$  exchanger isoform 1 takes part to the  $\text{Ca}^{2+}$ -related prosurvival pathway of SOD1 in primary motor neurons exposed to beta-methylamino-L-alanine. *Cell Commun. Signal.* **2022**, *20* (1), 8. Jan 12

PMID: 35022040; PMCID: PMC8756626

(31) Anzilotti, S.; Valsecchi, V.; Brancaccio, P.; Guida, N.; Laudati, G.; Tedeschi, V.; Petrozziello, T.; Frecentese, F.; Magli, E.; Hassler, B.; Cuomo, O.; Formisano, L.; Secondo, A.; Annunziato, L.; Pignataro, G. Prolonged NCX activation prevents SOD1 accumulation, reduces neuroinflammation, ameliorates motor behavior and prolongs survival in a ALS mouse model. *Neurobiol. Dis.* **2021**, *159*, No. 105480. Epub 2021 Aug 16. PMID: 34411705

(32) Anzilotti, S.; Valente, V.; Brancaccio, P.; Franco, C.; Casamassa, A.; Lombardi, G.; Palazzi, A.; Conte, A.; Paladino, S.; Canzoniero, L. M. T.; Annunziato, L.; Pierantoni, G. M.; Pignataro, G. Chronic exposure to l-BMAA cyanotoxin induces cytoplasmic TDP-43 accumulation and glial activation, reproducing an amyotrophic lateral sclerosis-like phenotype in mice. *Biomed. Pharmacother.* **2023**, *167*, No. 115503. Epub 2023 Sep 18. PMID: 37729728

(33) Chen, K.; Northington, F. J.; Martin, L. J. Inducible nitric oxide synthase is present in motor neuron mitochondria and Schwann cells and contributes to disease mechanisms in ALS mice. *Brain Struct. Funct.* **2010**, *214* (2–3), 219–34. Epub 2009 Nov 4. PMID: 19888600; PMCID: PMC3010349

(34) Drechsel, D. A.; Estévez, A. G.; Barbeito, L.; Beckman, J. S. Nitric oxide-mediated oxidative damage and the progressive demise of motor neurons in ALS. *Neurotox. Res.* **2012**, *22* (4), 251–64. Epub 2012 Apr 10. PMID: 22488161; PMCID: PMC4145402

(35) Gowing, G.; Dequen, F.; Soucy, G.; Julien, J. P. Absence of tumor necrosis factor-alpha does not affect motor neuron disease caused by superoxide dismutase 1 mutations. *J. Neurosci.* **2006**, *26* (44), 11397–402. Nov 1 PMID: 17079668; PMCID: PMC6674545

## ■ NOTE ADDED AFTER ASAP PUBLICATION

This article was published ASAP on June 22, 2024. The labels in Figure 3 have been updated and the corrected version was reposted on June 26, 2024.